Instantaneous Radio Spectra of Giant Pulses from the Crab Pulsar from Decimeter to Decameter Wavelengths

M. V. Popov,[1] A. D. Kuzmin,[2] O. M. Ul'yanov,[3] A. A. Deshpande,[4,5]
A. A. Ershov,[2] V. V. Zakharenko,[3] V. I. Kondratiev,[1]
S. V. Kostyuk,[1] B. Ya. Losovskiĭ,[2] and V. A. Soglasnov[1]

[1] *Astro Space Center, Lebedev Physical Institute, Russian Academy of Sciences, Profsoyuznaya ul. 84/32, Moscow 117997, Russia*

[2] *Pushchino Radio Astronomy Observatory, Astro Space Center, Lebedev Physical Institute, Russian Academy of Sciences, Pushchino, Moscow oblast', 142290 Russia*

[3] *Institute of Radio Astronomy, Ukrainian National Academy of Sciences, Krasnoznamennaya ul. 4, Kharkov 61002 Ukraine*

[4] *Raman Research Institute, C. V. Raman Av., Sadashivanagar Bangalore, 560 080 India*

[5] *Arecibo Observatory, HC03 Box 53995, Arecibo, 00612 Puerto Rico*

(Received December 17, 2005; Revised February 6, 2006)

The results of simultaneous multifrequency observations of giant radio pulses from the Crab pulsar, PSR B0531+21, at 23, 111, and 600 MHz are presented and analyzed. Giant pulses were detected at a frequency as low as 23 MHz for the first time. Of the 45 giant pulses detected at 23 MHz, 12 were identified with counterparts observed simultaneously at 600 MHz. Of the 128 giant pulses detected at 111 MHz, 21 were identified with counterparts observed simultaneously at 600 MHz. The spectral indices for the power-law frequency dependence of the giant-pulse energies are from -3.1 to -1.6. The mean spectral index is -2.7 ± 0.1 and is the same for both frequency combinations (600–111 MHz and 600–23 MHz). The large scatter in the spectral indices of the individual pulses and the large number of unidentified giant pulses suggest that the spectra of the individual giant pulses do not actually follow a simple power law. The observed shapes of the giant pulses at all three frequencies are determined by scattering on interstellar plasma irregularities. The scatter broadening of the pulses and its frequency dependence were determined as

$\tau_{sc} = 20(\nu/100)^{-3.5\pm0.1}$ ms, where the frequency ν is in MHz.

1. INTRODUCTION

The pulsar in the Crab Nebula, PSR B0531+21, was discovered by Staelin and Reifenstein [1] in 1968 as a result of detection of anomalously strong pulses. Such pulses were subsequently called giant. The peak flux in these pulses exceeds hundreds and thousand times the peak flux in an average pulse formed by synchronous integration of the pulsar signal with the neutron star rotation period, which is equal for the pulsar B0531+21 to approximately 33 ms. Giant pulses (GPs) of radio emission were detected in several pulsars: first millisecond pulsar B1937+21 [2, 3], millisecond pulsars J1824−2452 [4], B0540−69 [5], B1957+20, and J0218+4232 [6] as well as millisecond pulsar J1823−3021A in the globular cluster NGC 6624 [7]. GPs were detected in the usual pulsars B0031−07 [8], B1112+50 [9], and J1752+2359 [10]. In all these pulsars GPs are observed rather seldom, and their properties have still been poorly studied.

The properties of GPs have been studied in more detail for the Crab pulsar B0531+21 (see, e.g., a brief review of Hankins [11]) and first millisecond pulsar [12–14]. Together with a high peak flux density, which exceeds at decimeter wavelengths a hundred thousand janskys, GPs from the pulsar B0531+21 have an extremely short duration. At 5.5 GHz Hankins et al. [15] found in this pulsar outbursts shorter than 2 ns. Such nanopulses have a brightness temperature of radiation that exceeds 10^{37} K. Still higher brightness temperature (5×10^{39} K) have been obtained for GPs from the millisecond pulsar B1937+21 [14]. Thus, GPs suggest a highly efficient mechanism of radio emission, and the analysis of their properties can result in understanding the nature of this coherent mechanism.

An important characteristic of GPs is their radio spectrum. GPs from B0531+21 were detected at all frequencies where they were searched for. For the first time GPs were detected at 112 MHz [1]. Hankins [11] mentioned observing one GP at 15 GHz.

Of primary interest are simultaneous observations of GPs at several frequencies, when one can obtain instantaneous spectra of individual pulses. In 1999 Sallmen et al. [16] published the results of simultaneous observations of GPs from the pulsar B0531+21 at 1400 MHz (VLA) and 600 MHz (25-m radio telescope of Green Bank Observatory). Approximately 70% of GPs detected at 1400 MHz were also recorded at 600 MHz. The spectral indices

of such pulses are from −4.9 to −2.2. The same paper reports the results of simultaneous observations at 1.4 and 4.9 GHz. The spectral indices for these frequencies were from −4 to 0. Thus, though the average value of the GP spectral index was close to that for the components of the average pulse profile (according to Moffett [17], in the considered frequency band this value is −3.0), but instantaneous spectra of individual GPs varied in rather broad limits, indicating a complex character of the GP radio spectrum, which cannot be described by a simple power law.

In this paper we report the results of the analysis of instantaneous spectra of GPs in the radio emission from the pulsar B0531+21 that were measured in simultaneous observations at 23.23 MHz (UTR-2 radio telescope, Kharkov), 111.87 MHz (BSA radio telescope, Pushchino), and 600.0 MHz (64-m radio telescope, Kalyazin).

2. OBSERVATIONS AND DATA PROCESSING

The observations were carried out on November 24–26, 2003, within the framework of the international program of multifrequency studies of GP properties in the Crab pulsar. In addition to the radio telescopes mentioned in the Introduction, the GP observations were conducted also on the 100-m radio telescope at Effelsberg (8350 MHz), 76-m radio telescope of Jodrell Bank Observatory (1400 MHz), and Westerbork Synthesis Radio Telescope (1200 MHz). A complete analysis of the multifrequency observations will be presented in other publications.

2.1. 23 MHz

The observations at 23 MHz were conducted on the UTR-2 radio telescope. The radio telescope is T-shaped and consists of three segmented antennas: southern (S), northern (N), and western (W), corresponding to the directions from the UTR-2 phase center. The UTR-2 structure uses broadband Nadeenko vibrators, which receive radiation with the East–West linear polarization. The total number of the UTR-2 vibrators is 2040. For more details about UTR-2 and features of its system of amplifiers see [18, 19].

To solve our problem we have used a dual-channel reception system. The signal summed from the S and N (S+N) antennas was fed to the first channel of the receiver, while the

second channel was connected to the output of the western antenna (W). This usage of the antennas allowed us to have an additional criterion for the GP detection by comparison of the output signals from the two channels. We chose identical receiving frequencies for both channels; this allowed us to form the sum and difference beams for the (S+N) antenna and W antenna.

We have used the dual-channel Portable Pulsar Receiver (PPR), which was designed in the Laboratory of Raman Research Institute (Bangalore, India). The receiver has an internal rubidium standard and frequency synthesizer, due to which both channels operate synchronously. The receiver implements digital heterodyning of the intermediate frequency signals and four-level (two-bit) quantizing of the output signal with a time step of 325 ns. A detailed description of this receiver can be found on the Web site of Raman Research Institute [20].

The system noise temperature is determined by the Galactic background radiation in the main lobe of the antenna beam, by the radio emission of the Crab Nebula itself, and by the self-noise of the receiving system. According to Roger et al. [21], in the 23–24 MHz band the brightness temperature of the Galactic background toward the Crab Nebula is 40,000 K. The noise of the UTR-2 radio telescope adds 4000-5000 K. The contribution of the Crab Nebula to the noise temperature in this frequency band is about 3000 Jy. The nonthermal pointlike radio source (pulsar) contributes another 1000 Jy [22].

It is rather difficult to make an accurate calibration and estimation of the UTR-2 sensitivity toward the Crab pulsar. For the 23–24 MHz range and used UTR-2 configuration the Crab Nebula is a pointlike object. Therefore, when observing in the decameter range, we see fast scintillations on irregularities of the interplanetary plasma and ionosphere. We must also take into account the change in the radio telescope effective area due to tracking of the pulsar.

When estimating the actual UTR-2 sensitivity, we compared in the calibration mode the radio telescope response toward the pulsar with the response from the reference noise generator placed at the phase center of the radio telescope. A similar comparison was done in additional observations of the Galactic background near the Crab Nebula. The main beam of the radio telescope was shifted from the Crab Nebula by approximately 2° in four directions. To remove the effect of scintillations on the sensitivity estimate and to determine the background level correctly, we smoothed the data obtained during 2 h of the observations.

This approach allowed us to estimate more correctly the brightness temperature of the Galactic background near the directions toward the pulsar; according to our estimates, it is $50,000 \pm 4000$ K at the frequencies 23-24 MHz. With the additional noise from the Crab Nebula and pointlike source, we obtained an estimate of the noise toward the pulsar recalculated to flux density units, approximately 9000 Jy. With signal averaging over the reception band (1.5 MHz) and over time (0.26624 s) we obtained an estimate of the sensitivity, i.e., rms deviation in flux density units, 15 Jy in the mode of registration of individual GPs. We consider that the inaccuracy of this estimate, in view of the errors of calibration and influence of scintillations, does not exceed 30%.

The effect of radiowave dispersion was removed by the method of coherent dedispersion [23]. In the signal restoration we used the dispersion measure 56.757 pc/cm^3 taken from the Jodrell Bank Crab Pulsar Monthly Ephemeris [24]. At the frequency $f_0 = 23$ MHz in the used frequency band $\Delta f = 1.538$ MHz the dispersive pulse broadening in interstellar plasma for the pulsar dispersion measure 56.757 pc/cm^3 is $\Delta t = 52.5$ s. When restoring the signal by coherent dedispersion on the time interval T the data segment with the duration Δt will be lost at the beginning or end of the total time interval T, depending on whether dedispersion is applied to the lower or upper end of the frequency band Δf. Therefore, the time interval T on which dedispersion is implemented must appreciably (at least by a factor of two) exceed Δt. We performed dedispersion in ten passes, each time compensating one-tenth of the total dispersion measure. In such an approach the time interval T was 10.9052 s, and the time Δt for DM = 5.6757 pc/cm^3 was accordingly 5.253 s. The data file for the Fourier transform had a size of 33 554 432 elements. Since the expected magnitude of pulse scattering on interstellar plasma irregularities was several seconds, we analyzed the retrieved record of the signal with averaging over a time interval of 0.26624 s. Before the detection of the first obvious GP, the retrieved signal was examined by eye; then we applied an automatic procedure of isolation of suspicious events based on the calculation of the convolution of the restored signal with a template repeating the shape of the detected pulse. The formal search criterion was established at a level of $5\,\sigma$ for the values of the computed convolution. The subsequent analysis showed that using the criterion of detection at a level of $5\,\sigma$ yields the number of false GPs less than 10%. This analysis was conducted by comparing the number of events detected in the signal that was retrieved at the final value of the dispersion measure (56.757 pc/cm^3) with the number of events detected in the signal at an intermediate stage

of recovery, at the value of the dispersion measure 45.4 pc/cm^3.

The time alignment of the observations at 23 MHz was provided by injecting to the first channel of the receiver time markers bound to the time service of the observatory. The clock rate of the time service was checked before each observational session with GPS signals. The marker repetition period was 10 s, the marker duration was 20 ms, and for each whole minute an expanded marker with a duration of 100 ms was formed. The formal accuracy of the time alignment of the recorded data was about 0.1 ms. The effective GP width was 4.0 seconds. The actual accuracy of the time alignment of the detected GPs is determined by the duration of the leading edge of these pulses and makes about 1 s.

2.2. 111 MHz

The observations were carried out on the BSA transit radio telescope of Pushchino Radio Astronomy Observatory (Astro Space Center, Lebedev Institute of Physics) with the effective area at the zenith of about 15 000 m^2. The flux sensitivity of the system as measured on discrete sources and pulsars with the known flux was $\sigma_S \approx 200$ mJy/MHz s (toward a sky area with the brightness temperature 1000 K). One linear polarization was received. A 64-channel receiver with the channel bandwidth $\Delta f = 20$ kHz was utilized. The total frequency band was 1.28 MHz. The frequency of the first (highest frequency) channel was 111.87 MHz. The sampling interval was 8.2 ms. The time constant $\tau = 10$ ms. Individual pulses were recorded.

The processing of the observations was performed in automatic mode. The records were cleaned of interference, and interchannel compensation for the dispersion delay was applied. Pulses exceeding noise at a 5σ level were selected; their amplitude, phase, and pulse width were determined.

To confirm the pulse belonging to the pulsar, we processed the observational data with splitting into groups of different frequency channels; processing showed the presence of a pulse in each group and the expected dispersion delay. Another test was processing with varied dispersion measure. As expected for the pulsar, the pulse magnitude and signal-to-noise ratio are maximum at processing with the nominal dispersion measure DM = 56.757 pc/cm^3.

The flux density was calibrated against the observations of the pulsar B1919+21. For these two pulsars all the parameters of the BSA beam pointing are identical. We have used

12 sessions of observations of the pulsar B1919+21. The 111-MHz flux density of the pulsar B1919+21 was adopted to be 1.55 Jy.

At 111 MHz the time alignment of the observations was done with the rubidium standard of the observatory time service controlled by TV signals of the State Time and Frequency Standard. The timing accuracy was better than 100 μs. The measured effective pulse width due to scattering is 25 ms. The accuracy of the pulse arrival time at this frequency is also limited by the effect of scattering and is 2 ms.

2.3. 600 MHz

The observations at 600 MHz were conducted on the TNA-1500 radio telescope in Kalyazin. The radio emission was received in two channels with left-hand (LCP) and right-hand (RCP) circular polarizations. In each polarization channel two 4-MHz frequency bands (upper and lower side bands) were recorded. The central frequency is 600.0 MHz. The time resolution was 250 ns. The data were recorded on video cassettes in a two-bit binary code by means of the S2 recording system. The data were played back off-line after the observations in Astro Space Center of the Lebedev Institute of Physics on a specialized S2-RDR system, which had been designed in Astrophysical Data Processing Department. The equivalent system temperature is 1300 Jy in view of the contribution of the radio emission from the Crab Nebula [25]. To improve the sensitivity of the GP search, we averaged the signal over 256 points (32 μs), because at 600 MHz the temporal broadening of pulses due to radiowave scattering on interstellar plasma irregularities is about 50 μs. With this averaging the fluctuation sensitivity was 110 Jy (at a σ level). In the GP search we combined in a certain way the signals in four recorded channels, so the resulting minimum detectable GP peak flux was 420 Jy. The technique of processing and criteria of GP detection were described in our previous publication [26].

The time alignment of the 600-MHz observations was done with a hydrogen standard of the observatory time service controlled by TV signals of the State Time and Frequency Standard and by GPS signals. The timing accuracy was 0.1 μs. At this frequency the accuracy of the pulse time of arrival is limited by the effect of scattering and is 10 μs. The average GP profile at 600 MHz with a time resolution of 4 μs is presented in the figure.

Table 1. Observational data

Frequency, MHz	600.0	111	23.23
Time of the observations, h	36	0.25	12
Number of detected GPs	40 200	128	45
Number of identified GPs		21	12
τ_{sc}, ms	0.043 ± 0.005	15 ± 3	$3\,000 \pm 1\,000$
$S_{\rm min}^{\rm peak}$, Jy	420	60	75
$S_{\rm max}^{\rm peak}$, Jy	34 000	700	150
$E_{\rm max}$, Jy ms	2 000	17 000	600 000

3. RESULTS

The table lists main observational parameters: total observational time at each frequency, number of detected GPs, number of GPs at 111 and 23 MHz identified with counterparts at 600 MHz, pulse scatter-broadening $\tau_{\rm sc}$, minimum peak flux density of detectable GPs $S_{\rm min}^{\rm peak}$, maximum peak flux density of observed GPs $S_{\rm max}^{\rm peak}$, radiation energy of the strongest GP $E_{\rm max}$.

Three observational sessions were carried out. At 23 MHz the total duration of the sessions was about 1 300 000 pulsar periods. During this time 45 GPs (1 GP per approximately 30 000 pulsar periods) with peak flux densities exceeding 75 Jy, or with energies above 300 000 Jy ms, were recorded. No GPs were detected at 23 MHz during the time common with the 111-MHz observations.

In three observational sessions (about 4 min each) at 111 MHz, which included about 20 000 pulsar periods 128 GPs (approximately 1 GP per 160 pulsar periods) with peak flux densities exceeding 60 Jy, or with energies above 2000 Jy ms, were recorded. The energy of the strongest GP exceeds the energy of the average pulsar pulse by a factor of approximately 40–50.

The total duration of the observations in Kalyazin was 36 hours; 40 200 GPs (1 GP per approximately 100 pulsar periods) with peak flux density exceeding 420 Jy, or with energies above 25 Jy ms, were recorded; 518 of them were observed in time common with the 111-MHz observations.

The smaller number of GPs detected at low frequencies is due to a decrease in the peak

flux density of the observed GPs because of pulse scatter-smearing and increase in the brightness temperature of the Galactic background. Therefore, only the most intense GPs were detectable.

The figure shows examples of individual GPs at each frequency (left) and average GP profiles (right). In this figure the time resolution is 0.26624 s, 8 ms, and 4 μs for 23, 111, and 600 MHz respectively. The average GP profile at 23 MHz was obtained by averaging ten strongest pulses, which were time-aligned by the maximum of the convolution used in the GP search at this frequency. At 600 MHz the average GP profile was obtained by averaging all strong pulses with peak flux densities exceeding 1000 Jy. With such averaging individual pulses were aligned by a point at the leading edge for which the maximum deviation from the average value was less than 30% of the maximum amplitude of this pulse on the record averaged over a time interval of 4 μs. The shape of the average pulse in all three ranges is produced by scattering on interstellar plasma irregularities.

GPs were identified at different frequencies by coincidence of pulse arrival instants reduced for the dispersive delay to an infinitely high frequency with the dispersion measure 56.757 pc/cm^3. At 600 and 111 MHz we have identified 21 simultaneous GPs. The spectral indices in the frequency dependence of the energies of these GPs are from -3.1 to -1.6. The mean spectral index is -2.7 ± 0.1. For pulses observed at the detection limit the spectral index for these frequencies is -2.6. Since the majority of GPs detected at 600 and 111 MHz have remained unidentified, we can conclude that 95% of pulses detected at 600 MHz have spectral indices with respect to 111 MHz that are less steep than -2.6, while 85% of GPs detected at 111 MHz, have spectral indices steeper than -2.6.

The most interesting result of our observations is the detection of GPs at 23 MHz. To identify them with counterparts detected at 600 MHz we have supposed that GPs at 23 MHz that coincide with GPs at 600 MHz within 1-s interval are simultaneous. To reduce the number of spurious identifications with GPs at 600 MHz, which are detected approximately every 3 s, we identified events at 23 MHz only with strong pulses at 600 MHz, which exceeded the $10\,\sigma$ level (1100 Jy). For chance events only two identifications were expected. We identified 12 simultaneous events. The spectral indices in the frequency dependence of the energies of these identified GPs are from -3.1 to -2.5. The mean spectral index is -2.7 ± 0.1.

This value of the spectral index should be treated with caution, because it is subject to the

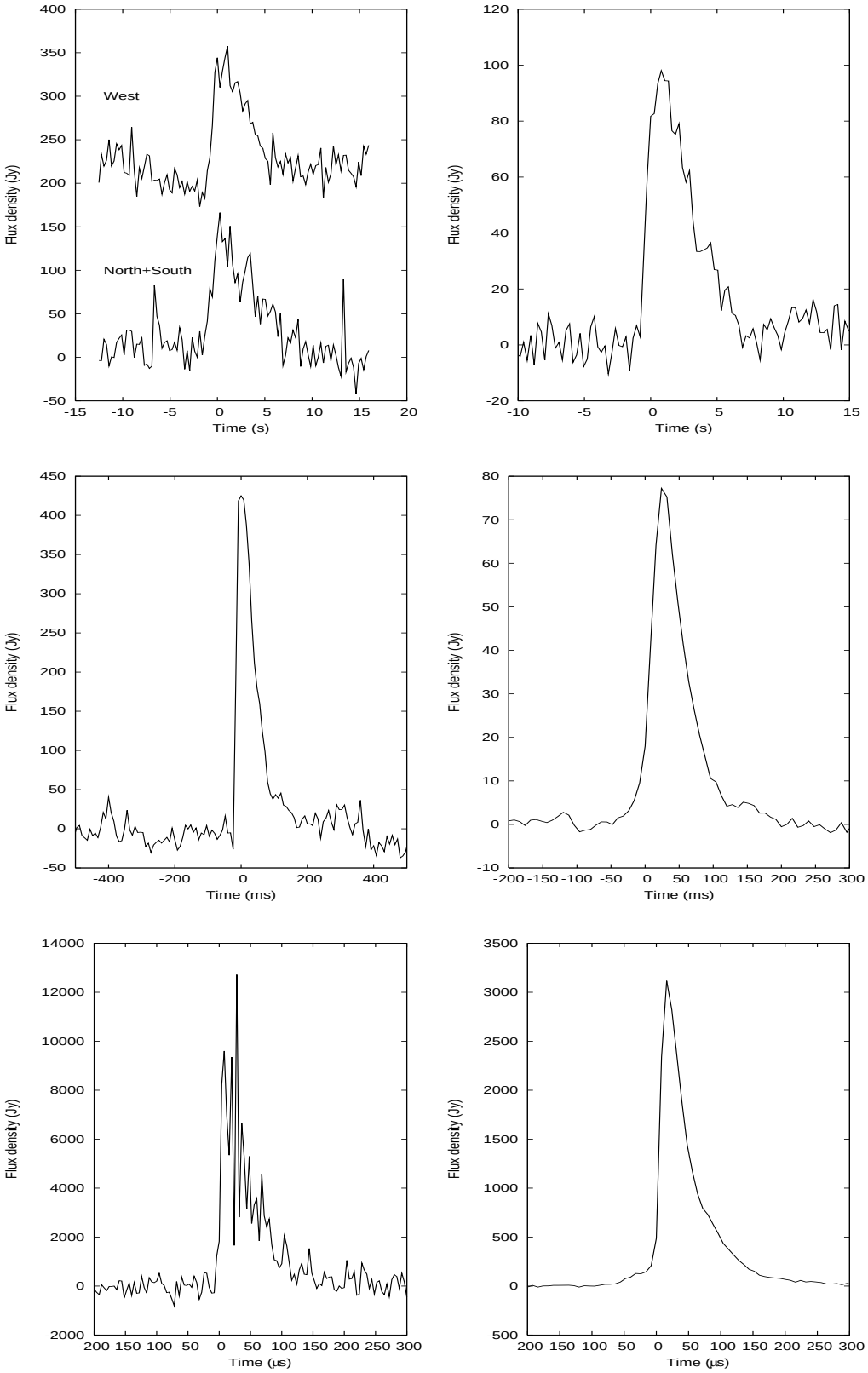

Figure 1. Upper left panel: a strong GP recorded at 23 MHz in two channels of the UTR-2 radio telescope. Short periodic splashes in the lower curve reflect 10-s markers injected into the receiving channel for time alignment. Upper right panel: average profile of GPs at 23 MHz obtained by averaging ten strongest pulses in the channel connected to the western arm of the UTR-2 antenna. Middle and lower panels: examples of an in-

selection effect. We compared at both frequencies a small number of pulses that exceeded the adopted detection limit. For pulses whose energies matched the detection limits at both frequencies the spectral index is -2.6, while pulses with spectral indices that appreciably differ from this value are unobservable at one or another frequency. Since during 12 h of simultaneous observations at 600 MHz we recorded about 1500 GPs with peak flux densities above $10\,\sigma$ and only 12 pulses were identified with the events at 23 MHz, the overwhelming majority of GPs detected at 600 MHz have spectral indices less steep than -2.6. On the other hand, we can assert on the same basis that a noticeable fraction of GPs detected at 23 MHz (about two thirds) have spectral indices steeper than -2.6.

The detection of giant pulses at 23 MHz has enabled us to expand the range for the measurement of the frequency dependence of pulse scatter-broadening to decameter waves. GPs are observed as very infrequent isolated pulses of a large intensity, which by far exceeds the mean level of the pulsar radio emission. This distinguishes GPs from a regular sequence of usual pulses, eliminates the effect of subsequent pulses, and enables measurements at low frequencies, where the pulse scatter-broadening exceeds the pulsar period.

The magnitude of the pulse scatter-broadening was determined by a comparison of the observed average GP profile with a model-scattered template representing the initial pulsar pulse. As a template a Gaussian pulse was taken. The template pulse was model-scattered by a convolution with a truncated exponent describing scattering on a thin screen. The observed pulsar pulse was least-square approximated with the obtained model-scattered pulse. The magnitude of scatter-broadening $\tau_{\rm sc}$, amplitude, width, and time delay of the template pulse were the sought parameters.

At 111 MHz the average GP profile was obtained from observations with a higher time resolution done on the days adjacent to the simultaneous observations. The table lists the results of the measurement of pulse scatter-broadening. A least squares fit yields the frequency dependence $\tau_{\rm sc} = 20(\nu/100)^{-3.5\pm0.1}$ (where $\tau_{\rm sc}$ is in ms, and ν is in MHz), which matches well broader band measurements of the frequency dependence of scattering for this pulsar [27]: $\tau_{\rm sc} = 22(\nu/100)^{-3.8\pm0.2}$.

4. CONCLUSION

We have performed simultaneous observations of giant pulses in the Crab pulsar (PSR B0531+21) radio emission at 600, 111, and 23 MHz. We have detected for the first time giant pulses at the lowest frequency 23 MHz. Thus, the mechanism of generation of giant pulses extends to the decameter frequency band. The mean spectral index α of the frequency dependence for the energy of identified pulses is identical in the 600–111 and 600–23 MHz ranges and is equal to -2.7. A considerable range of variations in the GP spectral indices and a large number of unidentified pulses suggest that the representation of instantaneous spectra of giant radio pulses of the pulsar B0531+21 by a simple power law does not describe the true shape of the radio spectrum of these pulses, which may have a complex form. We have measured pulse scatter-broadening and its frequency dependence: $\tau_{\rm sc} = 20(\nu/100)^{-3.5\pm0.1}$. The exponent of this power law differs from the values predicted either by the Kolmogorov model for the spectrum of irregularities of scattering plasma (-4.4) or by the Gaussian model (-4.0). We attribute this fact to a considerable contribution of the Crab Nebula itself to scattering of the pulsar radio emission.

ACKNOWLEDGMENTS

The authors thank K.G. Belousov and A.V. Chibisov for maintenance of the S2-RDR data playback system, to Yu.P. Ilyasov and V.V. Oreshko for their help with the observations on the 64-m Kalyazin radio telescope, to V.V. Ivanova and K.A. Lapaev for maintenance of the observations on the BSA radio telescope, and to A.D. Khristenko for the help with the observations on the UTR-2 radio telescope. This work was supported by the Russian Foundation for Basic Research (project codes 04-02-16384 and 05-02-16415) and Program of the Presidium of the Russian Academy of Sciences on Formation and Evolution of Stars and Galaxies. The authors thank the Ministry of Education and Science of Ukraine, which provided financial support of this work (contracts 729-2001 and F8/343-2004) and to Raman Research Institute (India) for manufacturing the PPR recorder.

---

1. D. H. Staelin and E. C. Reifenstein III, Science **162**, 1481 (1968).

2. A. Wolszczan, J. M. Cordes, and D. R. Stinebring, *Millisecond Pulsars*, eds S. P. Reinolds and D. R. Stinebring (Green Bank: NRAO, 1984), p. 63.
3. S. Sallmen and D. C. Backer, *Millisecond Pulsars. A Decade of Surprise*, eds A. S. Fruchter, M. Tavani, and D. C. Backer, ASP Conf. Ser. **72**, 340 (1995).
4. R. W. Romani and S. Johnston, Astrophys. J. **557**, L93 (2001).
5. S. Johnston and R. W. Romani, Monthly Notices Roy. Astron. Soc. **332**, 109 (2002).
6. B. C. Joshi, M. Kramer, A. G. Lyne, *et al.*, in *Young Neutron Stars and Their Environments*, IAU Symp. No. 218, eds F. Camilo and B. M. Gaensler (San Francisco: ASP, 2004), p. 68.
7. H. S. Knight, M. Bailes, R. N. Manchester, *et al.*, Astrophys. J. **625**, 951 (2005).
8. A. D. Kuz'min, A. A. Ershov, and B. Ya. Losovskii, Astron. Lett. **30**, 247 (2004).
9. A. A. Ershov and A. D. Kuz'min, Astron. Lett. **29**, 91 (2003).
10. A. A. Ershov and A. D. Kuzmin, Astron. and Astrophys. **443**, 593 (2005).
11. T. H. Hankins, *Pulsar Astronomy "— 2000 and Beyond*, eds M. Kramer, N. Wex, and R. Wielebinski, ASP Conf. Ser. **202**, 165 (2000).
12. I. Cognard, J. A. Shrauner, J. H. Taylor, and S. E. Thorsett, Astrophys. J. **457**, L81 (1996).
13. A. Kinkhabwala and S. E. Thorsett, Astrophys. J. **535**, 365 (2000).
14. V. A. Soglasnov, M. V. Popov, N. Bartel, *et al.*, Astrophys. J. **616**, 439 (2004).
15. T. H. Hankins, J. S. Kern, J. C. Weatherall, and J. A. Eilek, Nature **422**, 141 (2003).
16. S. Sallmen, D. C. Backer, T. H. Hankins, *et al.*, Astrophys. J. **517**, 460 (1999).
17. D. A. Moffett, Ph.D. Thesis (New Mexico Institute Mining and Technology, 1997).
18. A. V. Men', L. G. Sodin, N. K. Sharykin, et al., Antenny, No. 26, 15 (1978).
19. E. P. Abranin, Yu. M. Bruk, V. V. Zakharenko, and A. A. Konovalenko, Exp. Astron. **11**, 85 (2001).
20. http://www.rri.res.in/∼dspiral/ppr/hardware/hardware.htm.
21. R. S. Roger, C. H. Costain, T. L. Landecker, and C. M. Swerdlyk, Astron. and Astrophys. Suppl. Ser. **137**, 7 (1999).
22. A. L. Bobeiko, V. P. Bovkoon, S. Ya. Braude, *et al.*, Astrophys. Space Sci. **66**, 211 (1979).
23. T. H. Hankins, Astrophys. J. **169**, 487 (1971).
24. http://www.jb.man.ac.uk/∼pulsar/crab.html.
25. S. V. Kostyuk, V. I. Kondrat'ev, A. D. Kuz'min, et al., Astron. Lett. **29**, 387 (2003).
26. M. V. Popov, V. A. Soglasnov, V. I. Kondrat'ev, et al., Astron. Rep. **50**, 55 (2006).

27. A. D. Kuz'min, V. I. Kondrat'ev, S. V. Kostyuk, et al., Astron. Lett. **28**, 251 (2002).